Model for Olfactory Discrimination and Learning in *Limax* Procerebrum Incorporating Oscillatory Dynamics and Wave Propagation

B. ERMENTROUT,[1] JING W. WANG,[2] JORGE FLORES,[2] AND A. GELPERIN[2]
[1]*Department of Mathematics, University of Pittsburgh, Pittsburgh, Pennsylvania 15260; and* [2]*Biological Computation Research Department, Bell Laboratories, Lucent Technologies, Murray Hill, New Jersey 07974*

Received 28 April 2000; accepted in final form 5 December 2000

Ermentrout, B., Jing W. Wang, Jorge Flores, and A. Gelperin. Model for olfactory discrimination and learning in *Limax* procerebrum incorporating oscillatory dynamics and wave propagation. *J Neurophysiol* 85: 1444–1452, 2001. We extend our model of the procerebral (PC) lobe of *Limax*, which is comprised of a layer of coupled oscillators and a layer of memory neurons, each layer 4 rows by 20 columns, corresponding to the cell body layer (burster cells) and neuropil layer (nonburster cells) of the PC lobe. A gradient of connections in the layer of model burster cells induces periodic wave propagation, as measured in the PC lobe. We study odor representations in the biological PC lobe using the technique of Kimura and coworkers. Lucifer yellow injection into intact *Limax* after appetitive or aversive odor learning results in a band or patch of labeled cells in the PC lobe with the band long axis normal to the axis of wave propagation. Learning two odors yields two parallel bands of labeled PC cells. We introduce olfactory input to our model PC lobe such that each odor maximally activates a unique row of four cells which produces a short-term memory trace of odor stimulation. A winner-take-all synaptic competition enabled by collapse of the phase gradient during odor presentation produces a single short-term memory band for each odor. The short-term memory is converted to long-term memory if odor stimulation is followed by activation of an input pathway for the unconditioned stimulus (US) which presumably results in release of one or more neuromodulatory amines or peptides in the PC lobe.

INTRODUCTION

The computational function of coherent oscillations and synchronous firing is under investigation at a number of loci in the mammalian CNS, notably hippocampus (Czurko et al. 1999; Draguhn et al. 1998), cerebellum (Hartmann and Bower 1998; Mann-Metzer and Yarom 1999), cortex (Crook et al. 1997, 1998; Murthy and Fetz 1996), and thalamocortical circuits (Buzsaki 1991; Llinas et al. 1998). Oscillatory synchronization of activity in spatially dispersed cortical modules has been invoked as critical for feature binding during internal stimulus representation (Singer 1998; Singer and Gray 1995)

The olfactory bulb shows reliable and robust odor-evoked oscillatory activity (Adrian 1942; Delaney and Hall 1996; Dorries and Kauer 2000; Freeman 1991; Lam et al. 2000). In arthropods olfactory oscillations have been shown to result in synchronous firing of odor-responding interneurons (Heinbockel et al. 1998; Mellon and Wheller 1999; Wehr and Laurent 1999). The ubiquitous occurrence of olfactory oscillations (Gelperin 1999) and the extensive cellular studies of olfactory bulb (Shepherd 1999; Shipley and Ennis 1995) have prompted construction of a variety of structural models of olfactory bulb function incorporating oscillatory dynamics (Hendin et al. 1998; Li and Hopfield 1989; Linster and Gervais 1996; Meredith 1992; Taylor and Keverne 1991; White et al. 1992).

The procerebral (PC) lobe of the terrestrial mollusc *Limax* maximus is the major central site of odor processing and displays a number of design features in common with olfactory bulb (Gelperin 1999; see also Hildebrand and Shepherd 1997). These include oscillatory dynamics (Gelperin and Tank 1990; Kawahara et al. 1997) modified by behaviorally relevant odors (Gervais et al. 1996; Kimura et al. 1998c), circuits based on principal cells interacting with local inhibitory interneurons (Kleinfeld et al. 1994; Watanabe et al. 1998), continuous generation and connection of newly generated receptors after birth (Chase and Rieling 1986), postembryonic generation of olfactory interneurons (Zakharov et al. 1998), and modulation of circuit dynamics by both nitric oxide (Gelperin 1994) and carbon monoxide (Gelperin et al. 2000).

We have constructed a coupled oscillator model of the *Limax* PC lobe (Ermentrout et al. 1998). The model has two layers of units, each layer comprising 20 rows of four units, corresponding to the layers of burster cells and nonburster cells in the PC lobe. The four units in *row 1* correspond to the most apical part of the PC lobe, while the four units in *row 20* correspond to the most basal part of the PC. The model has a gradient of connection strengths between burster units so that it propagates activity waves, as measured in the PC lobe (Delaney et al. 1994). Recent evidence suggests that odor learning by *Limax* results in band-like regions of odor representation in the PC lobe (Gelperin 1999; Kimura et al. 1998a,b; Teyke and Gelperin 1999). Injection of intact *Limax* with Lucifer yellow (LY) after odor learning results in a band of LY-labeled cells in the PC lobe with the long axis of the band of labeled cells normal to the apical-basal axis of wave propagation. Learning two odors yields two parallel bands of la-

Address for reprint requests: A. Gelperin, Rm. 1C464, Bell Laboratories, 600 Mountain Ave., Murray Hill, NJ 07974 (E-mail: CNSAG@physics.bell-labs.com).

The costs of publication of this article were defrayed in part by the payment of page charges. The article must therefore be hereby marked "*advertisement*" in accordance with 18 U.S.C. Section 1734 solely to indicate this fact.

beled PC cells. We introduce olfactory input to our model PC such that each odor maximally activates a unique row of four cells which produces a long-term memory trace if odor stimulation is followed by activation of an input pathway for the unconditioned stimulus (US). Dynamics inherent in wave propagation suggests that similar but perceptually distinct odors result in closely spaced but distinct bands in the model PC. The model also has the property that if wave propagation is blocked, inputs from closely related odors address the same band in the model. This accords with recent work in honeybee showing that antennal lobe oscillations are necessary for discriminating closely related odors (Stopfer et al. 1997) and with electrophysiological results in *Limax* in which peritentacular nerve output becomes similar for related odors only when the PC oscillation and wave propagation are blocked (Teyke and Gelperin 1999).

METHODS

Labeling odor memory bands

In the first experiment, each slug was given one training trial in which it was induced to eat an agarose pellet containing starch, sucrose, and mint, an aversive odor. The 2.5% (wt/vol) agarose contained 4% (wt/vol) cornstarch, 10% (wt/vol) sucrose, and 0.01% (vol/vol) mint extract (McCormick). The slug was induced to initiate feeding movements by application of a solution containing 4% starch and 10% sucrose. The mint-containing agarose disk was placed in contact with the lips during ongoing feeding movements, resulting in ingestion of a substantial amount of the agarose pellet. This appetitive conditioning results in subsequent approach responses to mint odor, which prior to conditioning elicited aversive responses. Following the protocol of Kimura et al. (1998a), 20 min after completion of the appetitive training trial the slug was injected with 200 μl of 8% Lucifer yellow CH lithium salt (Sigma) in *Limax* saline. One hour later the slug was dissected and the PC lobes desheathed and photographed. Drawings were made as overlays from the scanned PC lobe photographs.

In the second experiment, we starved a group of 15 slugs weighing 2 g for 10 days and then applied potato odor-quinidine aversive conditioning as follows. Each slug was placed in a dry 15-cm Petri dish. After the slug started to crawl spontaneously, 1 ml of a 5% (wt/vol) solution of potato flakes in water was placed in front of the slug's head. Before the slug touched the source of potato odor ($\sim$10 s), 100 μl of a saturated solution of quinidine sulfate was applied to the oral area of the head. After 20 s the slug was rinsed with *Limax* saline and transferred to a clean chamber lined with moist filter paper. Control slugs given unpaired conditioning were treated similar to conditioned slugs except that after the 10-s potato-odor exposure the slug was gently moved to a clean Petri dish for 15 min before treatment with quinidine sulfate. Twenty minutes after the conditioning or control procedure, 200 μl of 0.1% (wt/vol) LY in *Limax* saline was injected into the hemocoel, where it distributed throughout the slug, turning it distinctly yellow. One hour after LY injection, the animal was anesthetized with cold and the brain harvested by fine dissection, followed by fixation in 4% (wt/vol) paraformaldehyde. Photographs were taken of the fixed preparations and scored for labeled cells using the following categories; 0 = no labeled cells, few = few scattered cells, cluster = group of labeled cells.

In a third experiment we used an aversive odor conditioning procedure previously shown to be effective (Sahley et al. 1981) and exposed the entire CNS to LY during memory consolidation as in the previous experiment. Aversive conditioning was applied to 26 slugs (1.0–2.2 g) selected for approach and feeding responses within 2 min to a piece of potato tuber (*Solanum tuberosum*) placed 1 cm in front of the slug. After feeding for 5 min, the slug was gently transferred to a Petri dish lined with filter paper moistened with 1% (wt/vol) quinidine sulfate. The slug was left in contact with quinidine for 20 min, after which it was injected with 0.8% (wt/vol) LY, Li, or K salt, in *Limax* saline, at a dosage of 100 μl/g body wt. One hour after injection of LY, the PC lobes were harvested by microdissection and examined with epifluorescence illumination in a compound microscope. Drawings were made of the distribution of labeled cells in the unfixed PC lobe and photographs taken with a CCD camera.

Modeling

Simulations of dynamical equations were made using custom software (XPP or XTC, available at http://www3.pitt.edu/~phase) running on a UNIX workstation. The output of the model was taken either as the spatial pattern of activity over the array of units or as the simulated voltage of individual units.

To account for the bilaterality of the lobe and the fact that in some circumstances bands occur on one side or the other, we will generalize our current model to include two distinct lobes. Experiments suggest that there are crossed inhibitory connections between the two lobes (Teyke and Gelperin 1999). Inhibitory connections can play two distinct roles in coupled oscillators. If the coupling strength is not too strong, then they can serve to synchronize the two lobes. This leads to a coherent traveling wave in which both lobes produce traveling waves. However, if the inhibition is too strong, then it is possible to suppress one side or the other depending on the initial conditions and local heterogeneities (White et al. 1998). Thus crossed inhibition plays two roles as follows: *1*) in the default mode of the model, it serves to synchronize the traveling waves between the two halves, and *2*) in "learning" mode when the oscillations synchronize, it can act to suppress one side or the other allowing asymmetric LY band formation.

In our previous paper (Ermentrout et al. 1998), we showed that a simple one-variable phase-model description was sufficient to model the traveling waves and the transition to synchrony. We continue that simplification in the present paper by using a single layer of oscillatory (bursting) cells. In addition, we add a layer of memory cells to represent the nonbursting neurons that take up the LY and encode the odor memory. The basic idea of the model is that the oscillatory cells act as gates to the inputs to the memory cells. Thus the memory cells will fire in the presence of inputs only during certain cycles of the oscillation. The memory cells suppress distant cells in the same layer (lateral inhibition) but only when they are active. Thus if there is a phase gradient in the oscillation, the suppression mechanism will not work since cells are never active at the same time. However, when the wave collapses to a synchronous oscillation, all the cells fire simultaneously in both lobes and the localization of odor bands becomes possible. Li and Hertz (2000) have devised a model that has some similar features for studying associative memory in the mammalian olfactory system. Their olfactory bulb layer plays a similar role to our oscillating layer and their olfactory cortex is like the "memory layer" in our model. However, there is no topographic organization in their model, the oscillations occur only during input, and there are no spatially organized waves.

The *Limax* model consists of a left and right lobe coupled with mutual inhibition. Each lobe consists of two layers of cells, the oscillatory layer (bursters) and the memory layer (nonbursters). The oscillatory layer consists of a two-dimensional array of coupled phase oscillators identical in form to our previous model. Since the oscillations produced by this system are always synchronized along the axis perpendicular to the direction of the waves, we will collapse the oscillatory layer to a single row of cells that either produces a wave or is synchronized. Figure 1 shows a schematic for the model. Since the details of how the traveling waves are produced in the oscillatory layer are not important, we simplify the model proposed in Ermentrout et al. (1998) by both collapsing the two-dimensional oscillatory

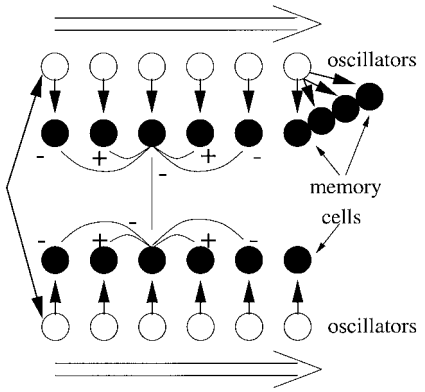

FIG. 1. Structure of the model. Each lobe is modeled by two layers. One layer consists of bursting oscillators which can produce waves or collapse to synchrony. The second layer consists of a network of nonbursting neurons whose inputs are gated by the oscillatory layer. This second layer has local excitatory connections and global inhibitory connections. Excitatory connections transversed to the direction of propagation (shown by the large arrows) are stronger than excitatory connections along the long axis of the lobe.

system to a single one-dimensional chain and imposing local frequency differences at the two ends sufficient to give a phase-gradient. In the simplified model, changing a single parameter collapses the gradient. The equation for the oscillator layer of the left lobe has the following form

$$\frac{d\theta_j^L}{dt} = \omega_j + H(\theta_{j+1}^L - \theta_j^L) + H(\theta_{j-1}^L - \theta_j^L) + G(\theta_j^R - \theta_j^L)$$

and a similar equation for the right lobe. The variables $\theta_j^{L,R}$ define the phase of the oscillation at spatial location j. The parameters ω_j are the intrinsic frequencies of the chain. We choose $\omega_2, \ldots, \omega_{N-1} = \omega$ to be constant. We choose $\omega_1 = \omega + H(-\mu)$ and $\omega_N = \omega + H(\mu)$ where μ is a parameter. We choose μ so that the apical end $j = 1$ oscillates slightly faster than the basal end $j = N$. This choice forces the chain to produce a traveling wave with a lag of μ between neighbors. The total lag from one end of the lobe to the other is $N\mu$. Setting $n = 20$, for example, with $\mu = \pi/10$ leads to a phase-gradient of one complete cycle. Setting $\mu = 0$ collapses the gradient and leads to synchronous oscillations. The functions H and G represent the interactions between the oscillators at neighboring spatial locations. We choose

$$H(\phi) = \sin\phi + \alpha(\cos\phi - 1)$$

and

$$G(\phi) = \sin\phi + \beta\cos\phi$$

The choice of G is somewhat arbitrary as long as $G'(0) > 0$ which ensures that the left and right lobes are synchronized with each other. Similarly, the choice of H is also very flexible with the only condition being $H'(\phi) > 0$ for ϕ between $\pm\mu$. In this paper, we pick $\beta = 0.5$, $\alpha = 0.5$, $\mu = \pi/10$, and $n = 21$ as the number of units. To collapse the gradient, we choose $\mu = 0$, forcing the network to synchronize.

Now we turn to the layer that is responsible for segmenting the input into a local spatial band. As shown in Fig. 1, we assume that this is driven by the oscillations and the input is only apparent to the cell at certain phases of the oscillation. The equation for the activity, $u_{j,k}^{L,R}$ of a cell at spatial location j, k on the left or right lobe is

$$\tau\frac{u_{j,k}^{L,R}}{dt} = -u_{j,k}^{L,R} + F(\nu_j^{R,L}I_{j,k}^{R,L} + \alpha_e s_{j,k}^{R,L} - \alpha_i z)$$

where

$$\nu_j^{R,L} = \exp(-5[1 + \cos\theta_j^{R,L}])$$

is the gating of the input due to the oscillation, $I_{j,k}^{L,R}$ is the input

$$s_{j,k}^{L,R} = \sum_{j',k'} w_{j',j,k',k} u_{j',k'}^{L,R}$$

is a local sum of the neighboring excitatory cells, and finally

$$\tau_z\frac{dz}{dt} = -z + \sum_{j,k}(u_{j,k}^L + u_{j,k}^R)$$

is a global negative feedback that is responsible for the winner-take-all (WTA) behavior of the network. Note that it includes components from both the left and the right lobes. The strength of the excitatory coupling along the direction perpendicular to the wave can be different from the coupling strength along the apical-basal (long) axis. The function, $F(u) = 1/\{1 + \exp[-5(u - 1.5)]\}$ is a standard "squashing" function used in neural nets. Note that the oscillatory gating depends only on j and not on k along the transverse axis of the lobe. This is because along the transverse axis all oscillators are synchronized; thus there is no reason to distinguish the oscillations in this direction.

We introduce a simplified model in which we look at the ability of the network to select between two competing inputs as a function of the phase-lag between the oscillatory gating. For this analysis, we look at

$$\tau\frac{du^R}{dt} = -u^R + F(\nu(\omega t)I^R + \alpha_e u^R - \alpha_i(u^R + u^L)) \quad (1)$$

$$\tau\frac{du^L}{dt} = -u^L + F(\nu(\omega t + \phi)I^L + \alpha_e u^L - \alpha_i(u^L + u^R)) \quad (2)$$

We will look at the ability of the network to determine the maximal input as a function of the parameter ϕ which is the phase-lag between the two driving oscillators and τ, the relaxation time of the network.

RESULTS

Lucifer yellow labels odor memory bands

An example of a unilateral LY-labeled band of PC lobe neurons resulting from single trial appetitive odor conditioning is shown in Fig. 2, *A* and *B*. The band of LY-labeled cells in the right PC lobe is oriented approximately normal to the apical-basal axis of wave propagation. The unilateral nature of the LY-labeled odor memory band strongly suggests some form of bilateral interaction which results in the dominance of the right side in this animal for storing odor memories. The learning-associated LY labeling occurs in half the animals on the right side and in half the animals on the left side.

Of the 10 slugs conditioned with potato-quinidine pairings in *experiment 2*, five (50%) showed a cluster of labeled cells in either the right or the left PC lobe (Table 1). The remaining five conditioned slugs had either a few scattered cells or no labeled cells in their PC lobes. Of the five control slugs, one (20%) showed a cluster in one PC lobe. The 15-min interval between potato odor and quinidine treatment may not be long enough to obviate learning in all slugs.

We performed a third experiment in an attempt to obtain more dramatic odor conditioning-dependent labeling of PC neurons. Of the 26 slugs given one trial of aversive odor conditioning in *experiment 2*, 16 (62%) had either a band or a patch in a PC lobe (Table 2). All but one slug had labeling in only the right PC lobe (6 of 15, 40%) or only the left PC lobe (9 of 15, 60%). Figure 3 shows examples of a band and a patch. We identified a band as a group of LY-labeled PC neurons with the length of the long axis of the region enclosing the labeled cells >2 times the length of the short axis (Fig. 3*D*) while a

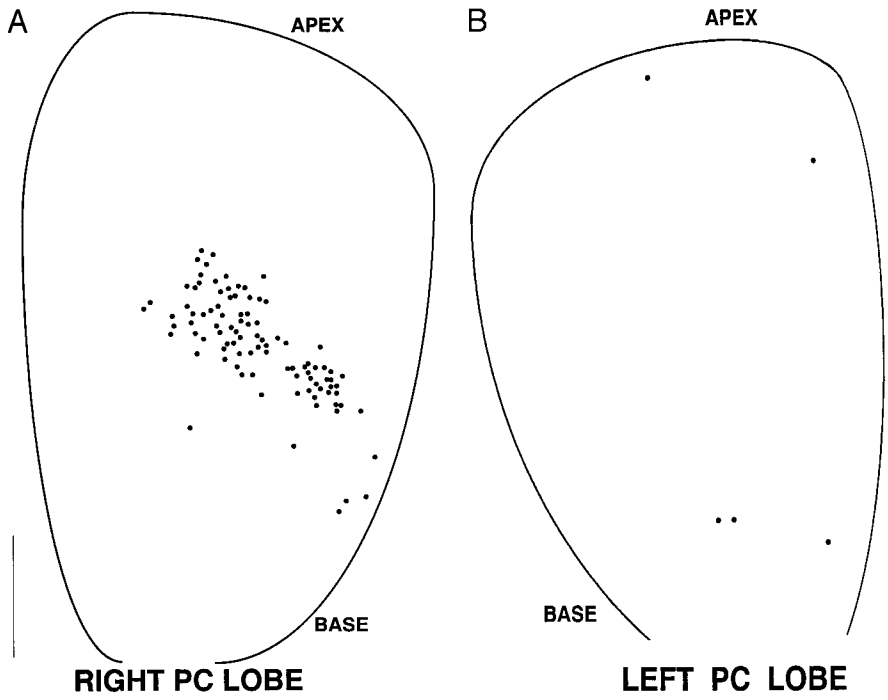

FIG. 2. Drawings of Lucifer yellow-labeled neurons made from photomicrographs of right and left procerebral lobes from a slug given one trial appetitive odor conditioning. The starved slug was induced to start feeding with a solution of sucrose and starch. After feeding movements were initiated, an agar pellet containing sucrose, starch, and mint extract was gently positioned in front of the slug contacting the lips, at which point the slug ingested a quantity of the agar pellet containing the mint odor. After this single odor training trial, the animal was injected with Lucifer yellow as described in the text and the brain examined with fluorescence microscopy for labeled neurons. The PC lobes showed the only significant staining in the CNS. Scale bar is 100 μm.

patch is a group of LY-labeled PC neurons with the long axis of the region enclosing the labeled cells $\leq$2 times the length of the short axis (Fig. 3*B*). In five of six cases (83%), the long axis of the LY-labeled band was parallel to the wave front of the activity wave which propagates from apex to base.

The LY is present in the somata of the labeled cells contained in membrane-bound vesicles, as determined by two-photon laser scanning microscopy (Denk et al. 1994). We also determined that the LY-labeled cells are nonburster (NB) neurons, the major class of interneurons in the PC lobe, rather than burster (B) neurons. B neurons are responsible for the oscillation of the local field potential and the wave-like propagation of activity from apex to base of the PC lobe (Delaney et al. 1994; Gelperin and Tank 1990; Kleinfeld et al. 1994). The LY-labeled cells have only one neurite which projects from the soma directly to the PC neuropil, characteristic of NB cells (data not shown). B cells have two or more neurites which project in the plane of the cell body layer and do not invade the PC neuropil (Wang et al. 2001). The unilateral nature of the LY labeling is a striking and unexpected feature which may derive from crossed inhibition between right and left odor processing streams, as recently demonstrated in the *Limax* nose-brain preparation (Teyke et al. 2000). The regional localization of LY-labeled PC neurons, particularly in band-like clusters with the long axis of the band parallel to the front of the propagating activity wave, prompted us to extend our model of the PC lobe to exhibit odor learning with storage of odor memories in bands of PC cells.

TABLE 1. *Learning-dependent Lucifer yellow labeling of neurons in the Limax procerebral lobe*

Slug	Paired/Unpaired	Right PC Lobe	Left PC Lobe
1	P	Few	Cluster
2	P	0	0
3	P	0	0
4	P	Few	Cluster
5	P	0	Cluster
6	P	Few	Few
7	P	Few	Cluster
8	P	Few	Few
9	P	Cluster	0
10	P	0	Few
1	U	Cluster	Few
2	U	Few	Few
3	U	0	0
4	U	Few	0
5	U	Few	Few

Cluster, five or more labeled cells in a contiguous group; Few, less than five single isolated cells; 0, no labeled cells.

Model for odor learning

The network, as before, begins with a chain of locally coupled oscillators with a gradient of coupling strengths so that at rest the network propagates a periodic wave with wavelength equal to the chain length (PC length). We obtain synchrony in response to odor input by nulling the coupling gradient. We assume that memory bands arise from neurons within the PC becoming more active in the presence of odor input and turning on some long-term process to store the odor memory due to US-triggered neuromodulation. The PC lobe contains several amine and peptide neuromodulators among the 21 different neurotransmitters found in the PC lobe (Gelperin 1999).

Model description

The model works as follows. During the generation of waves, if odor inputs come in, then each cell in the memory layer sees the inputs at different times due to the phase gradient. Thus no single cluster of cells can suppress all the others since it will be active at a different time in the cycle than the others. However, if the oscillatory network synchronizes, then all the active clusters are available for suppression at the same time and a "winner" emerges. It is important to point out that oscillations are not required for WTA. There are many simple

TABLE 2. *Odor conditioning induces Lucifer yellow labeling of neurons in the Limax procerebral lobe*

Slug	Right PC Lobe	Left PC Lobe
1	Cluster	0
2	0	0
3	0	Stripe
4	Stripe	0
5	0	0
6	Cluster	0
7	0	0
8	0	Cluster
9	0	0
10	Stripe	0
11	0	0
12	0	0
13	Stripe	0
14	0	Stripe
15	0	Cluster
16	Cluster	0
17	0	0
18	Cluster	Stripe
19	Cluster	0
20	0	0
21	0	Cluster
22	0	0
23	0	Cluster
24	Cluster	0
25	Stripe	0
26	0	0

All slugs given paired training with potato odor and quinidine taste. Cluster, contiguous group of labeled cells with major axis of group < twice the minor axis; Stripe, contiguous group of labeled cells with major axis > twice the minor axis; 0, no labeled cells.

networks without oscillations that can implement WTA behavior. However, if there are oscillations, then, by keeping them desynchronized (as through a phase-gradient), every point in the network is available for excitation at different points in the cycle. By transiently synchronizing the network, we enable it to select a unique spatial region to represent the input and presumably perform a useful computation. The other advantage of oscillations over a static WTA network is that it is simple to switch between behavior which selects a single most salient stimulus (during synchrony) to behavior allowing all inputs to have an effect (during waves).

As a first simulation we consider a pared down model representing the two sides of the *Limax*—that is, we collapse the right and left lobes to two points to illustrate the competition during synchrony. We ask under which circumstances a selection between two inputs can be made if they are not perfectly synchronized. We simulate *Eqs. 1* and *2* with the input to the right lobe slightly larger than that to the left. If the phase separation of the two oscillators is small enough, then the input to the left will be suppressed. We arbitrarily define suppression to mean that the response of u^L is <30% of that of u^R at their respective peaks. We choose $\omega = 0.2$ for the driving oscillations. Suppose that $\tau = 1$. Then if $\phi < 0.4$, then u^R will be selected and u^L suppressed. For each τ, there is a range of ϕ such that u^L will be suppressed. The maximum such ϕ is called the critical ϕ. Figure 4 shows a plot of the critical value of ϕ as a function of the relaxation constant of the network. If the network responds quickly, then the oscillations must be very close to synchrony in order to make a selection. This is because if the duration of the response of the network is quite short then suppression can only occur in a limited time window. On the other hand, if the duration of the network response is too long lasting, then the magnitudes of patterns are both small. Due to these factors there is an optimal response time for the network in which suppression takes place over a wide time window without undue reduction in response magnitude.

The previous simulation shows how gating the inputs can enable suppression between two sides if the timing is close enough. Since the left and right lobes are closely synchronized even during wave generation, it is clear that selection of one side or the other can readily occur through this mechanism.

We now turn to the full model. We ask whether spatial localization can occur and whether there will be bands. First, we remark that in a WTA network, there is no a priori reason why there should be bands. In fact, one expects only small clusters of cells to be selected. In particular, since the oscillations are always synchronous perpendicular to the direction of the traveling wave, the competition is "fiercest" in this direction. Thus there must be constraints on the connections in the

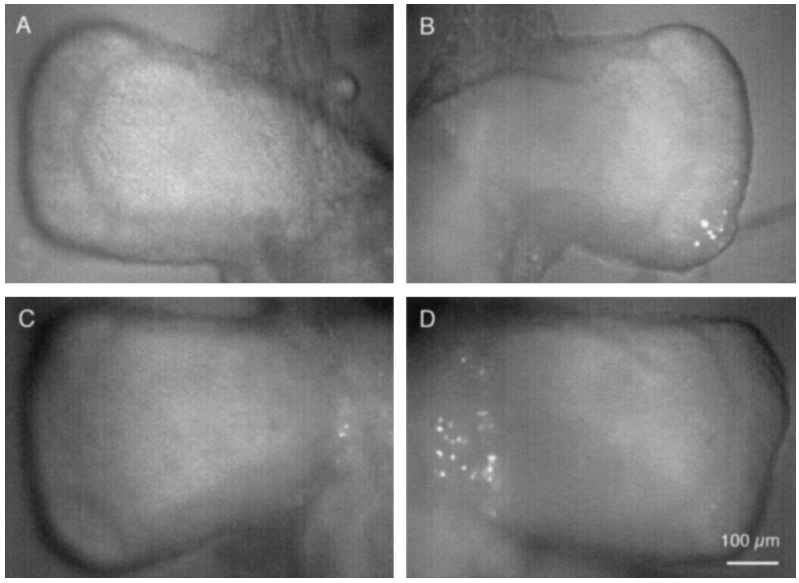

FIG. 3. Lucifer yellow-labeled neurons in the procerebral lobe of *Limax* after odor conditioning. *A* and *B*: left and right procerebral lobes of a slug given odor conditioning as described in the text and then injected with Lucifer yellow. A cluster of labeled cells is evident in the apical region of the right procerebral lobe (*B*), while the left procerebral lobe shows no labeled cells (*A*). *C* and *D*: left and right procerebral lobes from a different slug also given odor conditioning. A band-like area of labeled cells is present in the basal region of the right procerebral lobe (*D*), while only a few scattered labeled cells are found in the left procerebral lobe (*C*).

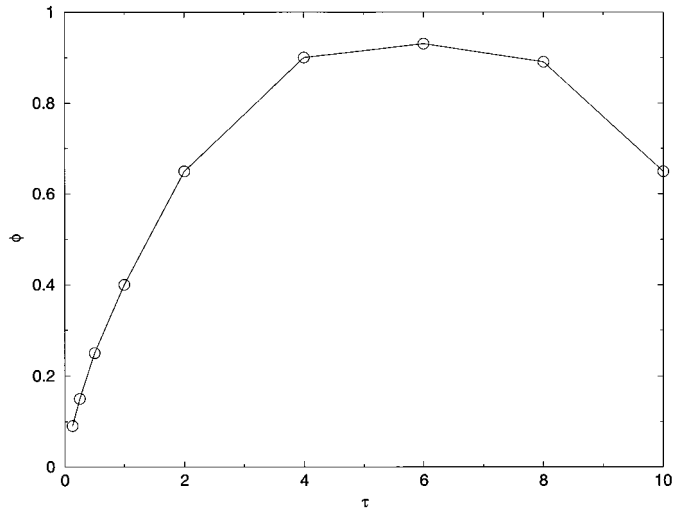

FIG. 4. Minimal phase-difference ϕ required to select a winner as a function of the time constant of the network. Parameters are $\alpha_e = \alpha_i = 1$, $F(u) = 1/\{1 + \exp[-5(u - 1.5)]\}$, $v(\omega t) > \exp\{-5[1 - \cos(\omega t)]\}$ with $\omega = 0.2$.

network and perhaps on the inputs. We suggest that there are relatively strong excitatory connections along the transverse direction and that the odor inputs to the lobe are similar in strength along this direction. If we make this assumption, then there is tendency for bands to occur even if the inputs are not identical. One of the consequences of tight coupling along the direction of the bands is that a band will form at a position *j* even if a single input to another region is larger than any of the inputs to the winning band. This is because of the cooperative effect of the coupling across the band. Figure 5 shows a sample of the times series from six spatial regions from a 20×4 array of cells. The wave propagates down the long axis of the array. The first four graphs show the activity of the four cells belonging to the winning pattern before (to the left of the top vertical arrow) and after the wave collapses to synchronous activity. Note the low activity in one of the units $u_{4,2}$ until the wave collapses. Then, after the bands in other spatial locations are suppressed, the activity in unit $u_{4,2}$ is enhanced. Two units from a suppressed region ($u_{1,9}$, $u_{4,9}$) are shown before and after the collapse of the wave. After the phase gradient collapses, the activity in both unit $u_{1,9}$ and unit $u_{4,9}$ is completely suppressed as is all activity in all spatial regions except the winning band.

Figure 6 shows the space-time evolution of the first row of cells along the long axis of one lobe. Inputs come to cells in *positions 1*, *2*, and *9*. After the wave collapses (shown by the >>>), only cells in the second position persist in their activity.

DISCUSSION

Two types of experimental results indicate that the PC lobe is involved in storing information related to odor learning. First, LY injection 20 min after a single odor training trial leads to bands or patches of labeled PC neurons. The LY labeling of PC neurons does not occur with odor and quinidine exposures timed to obviate learning (Kimura et al. 1998c). Second, if slugs are given aversive odor training and then responses to the trained odor measured by imaging the PC lobe using an in vitro nose-brain preparation, phase-specific depolarization in a band-shaped region of the PC lobe can be observed (cf. Fig. 6 in Kimura et al. 1998c). The phase-specific band of depolarization is seen in response to the conditioned odor but not to a control odor.

The learning-specific LY labeling of PC lobe neurons occurs in response to both aversive odor conditioning (cf. Figs. 2 and 3 and Kimura et al. 1998c) and appetitive conditioning (Fig. 1 in Gelperin 1999). The memory trace set up by *Limax* odor conditioning transforms from a short-term to long-term form (Sekiguchi et al. 1997, 1991; Yamada et al. 1992) as found in other species (Dubnau and Tully 1998; Squire 1987). The endocytosis-like event which results in LY filled vesicles in the somata of bands of NB neurons may be related to activation by the US (quinidine) of the biochemical cascade which transforms a short-term memory into a long-term form (Abel and Kandel 1998). Quinidine application may lead to release of a neuromodulatory transmitter in the PC, which contains 21 different neurotransmitter candidates (Gelperin 1999), includ-

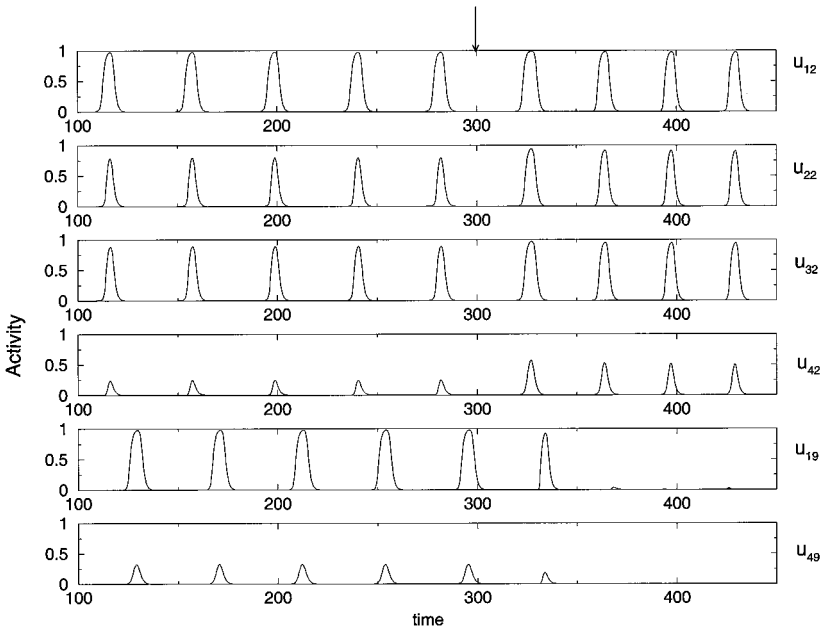

FIG. 5. Activity of units both within a single band $u_{1,2}$, $u_{2,2}$, $u_{3,2}$, $u_{4,2}$ as well as in a different band $u_{1,9}$, $u_{4,9}$ before and after the collapse of the phase-gradient. Arrow shows the time at which the gradient is collapsed. Since it takes a small but finite time for the entire oscillatory layer to synchronize, there is residual activity after the collapse begins, but this lasts at most one cycle.

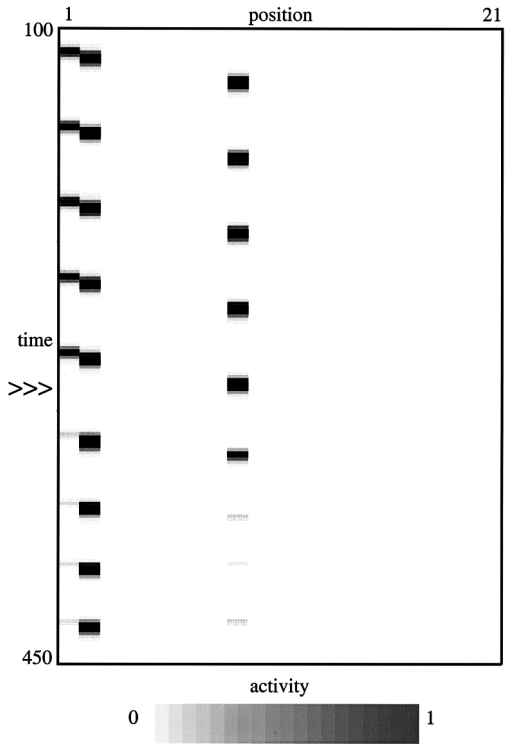

FIG. 6. Plot of the activity of all cells in one row of the network. >>> depicts the time at which the gradient collapses.

ing serotonin (but see Teyke 1996). The odor-learning-specific LY labeling of NB cells rather than B cells may derive from the fact that odor input fibers connect with the neurites of PC neurons only in the neuropil, which contains NB cell neurites but not B cell neurites (Wang et al. 2001; Watanabe et al. 1998).

The band of units in the model which forms an odor memory trace is a central representation of the learned odor which can be associated with either a positive or a negative behavioral response to the learned odor. The odor memory representation in the model PC may be coupled to changes in premotor circuitry located elsewhere to determine the nature of the behavioral response to the learned odor, as in the original *LIMAX* model (Gelperin et al. 1985). Both appetitive and aversive odor conditioning result in LY-labeled bands of neurons in the PC lobe. The LY-labeled neurons take up the dye due to membrane internalization events coupled to synaptic events which set up the odor memory, while in the model learning directly modifies synaptic strengths so that subsequent presentations of the learned odor produce unique localized patterns of activity in the PC. The link between synaptic modifications due to learning and membrane internalizations at the soma remains to be determined.

Wave propagation is blocked in the model by nulling the phase gradient. This yields synchronous oscillation of the entire mode PC. Only during synchronous activity can a selection of units most strongly driven by an odor input be made and competition occur to implement the WTA interaction resulting in a single band representing a single odor in the model PC. Wave propagation is blocked in the biological PC by treatments which block both wave propagation and synchronous oscillation, such as nitric oxide synthesis inhibitors. Under these conditions, when nitric oxide synthesis is blocked in vivo, no odor learning occurs (Teyke 1996).

The relation between perceptual and chemical similarity of odors and the spatial contiguity of their odor memory bands remains to be determined. If *Limax* is trained sequentially first with odor A and then with odor B, two LY-labeled bands are found in the same PC lobe (Kimura et al. 1998c). For carrot and cucumber odors, the bands are separated by about half the apical-basal extent of the PC lobe (cf. Fig. 13 in Kimura et al. 1998a). Using an in vitro nose-brain preparation, two closely related odors (apple variety A versus apple variety B) are not clearly discriminated from each other when the PC lobe oscillation and wave propagation are suppressed pharmacologically (Teyke and Gelperin 1999). We suggest that closely related odors are stored in spatially contiguous regions of the PC lobe and further, that in the absence of oscillatory dynamics and wave propagation, two similar odors with minimal spatial separation of their PC representations will no longer be discriminated from each other. This has also been observed in behavioral measurements of odor discrimination in honeybees after pharmacological suppression of antennal lobe oscillations (Stopfer et al. 1997). The storage of odor representations in spatially separated bands in the *Limax* PC lobe may be analogous to spatial segregation of odor representations in groups of glomeruli (Friedrich and Korsching 1997; Joerges et al. 1997; Vickers et al. 1998), which is also modified by associative learning (Faber et al. 1999).

A striking feature of the LY labeling of odor memory bands is the unilateral nature of the labeling in spite of bilateral odor exposure. This may result from the lateralized access of olfactory afferents to the PC lobe ipsilateral to a given nose in combination with crossed inhibition between right and left odor processing streams. Using the odor elicited peritentacular nerve discharge as a surrogate signal for appetitive odor responses (Peschel et al. 1996), clear evidence was obtained for right-left inhibition when the right superior nose was stimulated with known attractive odor A and simultaneously the left superior nose was stimulated with known attractive odor B (Teyke et al. 2000). This crossed inhibition between left and right odor processing streams resulting in unilateral odor memory storage could result in doubled odor memory storage capacity if one PC lobe is used for memory storage after the other PC lobe has stored the maximum number of odor memories consistent with accurate discrimination and recall.

The mechanism of learning-dependent LY uptake into the somata of procerebral NB neurons is unknown. There are demonstrations of activity-dependent LY uptake in a variety of neural tissues (Wunderer et al. 1989; Zimmerman 1986; Zinkl et al. 1990), although the nature of the activity leading to LY uptake is not known (Page et al. 1994; Sarthy et al. 1982). Uptake of LY into membrane-bound vesicles occurs at the somata of PC nonburster neurons, perhaps as a concomitant of somatic release and recycling of synaptic vesicles. Somatic exocytosis of transmitter vesicles has been shown for an identified dopamine neuron in the aquatic snail *Planorbis* (Anderson et al. 1999; Chen et al. 1995) and somatostatin-containing neurons in the terrestrial snail *Helix* (Darbon et al. 1996). The somatic vesicles of somatostatin-containing *Helix* neurons incorporated the fluorescent dye FM1–43 after producing trains of action potentials, confirming that spike-triggered exocytosis and vesicle recycling occurred at the soma. Learning-induced

internalization of surface proteins such as cell adhesion molecules (Bailey et al. 1997; Martin and Kandel 1996) is another candidate mechanism for learning-induced internalization of LY.

Portions of this study were supported by National Science Foundation Grant DMS-9972913 to B. Ermentrout and National Institute of Mental Health Grants MH-47150 to B. Ermentrout and MH-56090 to A. Gelperin.

REFERENCES

ABEL T AND KANDEL ER. Positive and negative regulatory mechanisms that mediate long term memory storage. *Brain Res Rev* 26: 360–378, 1998.

ADRIAN ED. Olfactory reactions in the brain of the hedgehog. *J Physiol (Lond)* 100: 459–473, 1942.

ANDERSON BB, CHEN G, GUTMAN DA, AND EWING AG. Demonstration of two distributions of vesicle radius in the dopamine neuron of Planorbis corneus from electrochemical data. *J Neurosci Meth* 88: 153–161, 1999.

BAILEY CH, KAANG B-K, CHEN M, MARTIN KC, LIM C-S, CASADIO A, AND KANDEL ER. Mutation in the phosphorylation sites of MAP kinase blocks learning-related internalization of apCAM in Aplysia sensory neurons. *Neuron* 18: 913–924, 1997.

BUZSAKI G. The thalamic clock-emergent network properties. *Neuroscience* 41: 351–364, 1991.

CHASE R AND RIELING J. Autoradiographic evidence for receptor cell renewal in the olfactory epithelium of a snail. *Brain Res* 384: 232–239, 1986.

CHEN G, GAVIN PF, LUO G, AND EWING AG. Observation and quantitation of exocytosis from the cell body of a fully developed neuron in Planorbis corneus. *J Neurosci* 15: 7747–7755, 1995.

CROOK SM, ERMENTROUT GB, AND BOWER JM. Spike frequency adaptation affects the synchronization properties of networks of cortical oscillators. *Neural Comp* 10: 837–854, 1998.

CROOK SM, ERMENTROUT GB, AND VANIER MC. The role of axonal delay in the synchronization of networks of coupled cortical oscillators. *J Comp Neurosci* 4: 161–172, 1997.

CZURKO A, HIRASE H, CSICSVARI J, AND BUZSAKI G. Sustained activation of hippocampal pyramidal cells by 'space clamping' in a running wheel. *Eur J Neurosci* 11: 344–352, 1999.

DARBON P, MONNIER Z, BRIDE M, CREST M, GOLA M, MARIANNEAU G, AND MATH F. Antibody-coated electrodes for detecting somatic exocytosis of somatostatin-like material in *Helix* neurons. *J Neurosci Meth* 67: 197–201, 1996.

DELANEY KR, GELPERIN A, FEE MS, FLORES JA, GERVAIS R, TANK DW, AND KLEINFELD D. Waves and stimulus-modulated dynamics in an oscillating olfactory network. *Proc Natl Acad Sci USA* 91: 669–673, 1994.

DELANEY KR AND HALL JB. An in vitro preparation of frog nose and brain for the study of odour-evoked oscillatory activity. *J Neurosci Meth* 68: 193–202, 1996.

DENK W, DELANEY KR, GELPERIN A, KLEINFELD D, STROWBRIDGE BW, TANK DW, AND YUSTE R. Anatomical and functional imaging of neurons using 2-photon laser scanning microscopy. *J Neurosci Meth* 54: 151–162, 1994.

DORRIES KM AND KAUER JS. Relationships between odor-elicited oscillations in the salamander olfactory epithelium and olfactory bulb. *J Neurophysiol* 83: 754–765, 2000.

DRAGUHN A, TRAUB RD, SCHMITZ D, AND JEFFERYS JGR. Electrical coupling underlies high-frequency oscillations in the hippocampus in vitro. *Nature* 394: 189–192, 1998.

DUBNAU J AND TULLY T. Gene discovery in *Drosophila*: new insights for learning and memory. *Annu Rev Neurosci* 21: 407–444, 1998.

ERMENTROUT B, FLORES J, AND GELPERIN A. Minimal model of oscillations and waves in the *Limax* olfactory lobe with tests of the model's predictive power. *J Neurophysiol* 79: 2677–2689, 1998.

FABER T, JOERGES J, AND MENZEL R. Associative learning modifies neural representations of odors in the insect brain. *Nature Neurosci* 2: 74–78, 1999.

FREEMAN WJ. Nonlinear dynamics in olfactory information processing. In: *Olfaction: A Model System for Computational Neuroscience*, edited by Davis JT and Eichenbaum H. Cambridge, MA: MIT Press, 1991, p. 225–249.

FRIEDRICH RW AND KORSCHING SI. Combinatorial and chemotopic odorant coding in the zebrafish olfactory bulb visualized by optical imaging. *Neuron* 18: 737–752, 1997.

GELPERIN A. Nitric oxide mediates network oscillations of olfactory interneurons in a terrestrial mollusc. *Nature* 369: 61–63, 1994.

GELPERIN A. Oscillatory dynamics and information processing in olfactory systems. *J Exp Biol* 202: 1855–1864, 1999.

GELPERIN A, FLORES J, RACCUIA-BEHLING F, AND COOKE IRC. Nitric oxide and carbon monoxide modulate oscillations of olfactory interneurons in a terrestrial mollusk. *J Neurophysiol* 83: 116–127, 2000.

GELPERIN A, HOPFIELD JJ, AND TANK DW. The logic of *Limax* learning. In: *Model Neural Networks and Behavior*, edited by Selverston AI. London: Plenum, 1985, p. 237–261.

GELPERIN A AND TANK DW. Odor-modulated collective network oscillations of olfactory interneurons in a terrestrial mollusc. *Nature* 345: 437–440, 1990.

GERVAIS R, KLEINFELD D, DELANEY KR, AND GELPERIN A. Central and reflex neuronal responses elicited by odor in a terrestrial mollusc. *J Neurophysiol* 76: 1327–1339, 1996.

HARTMANN MJ AND BOWER JM. Oscillatory activity in the cerebellar hemispheres of unrestrained rats. *J Neurophysiol* 80: 1598–1604, 1998.

HEINBOCKEL T, KLOPPENBURG P, AND HILDEBRAND JG. Pheromone-evoked potentials and oscillations in the antennal lobes of the sphinx moth *Manduca sexta*. *J Comp Physiol [A]* 182: 703–714, 1998.

HENDIN O, HORN D, AND TSODYKS MV. Associative memory and segmentation in an oscillatory neural model of the olfactory bulb. *J Comp Neurosci* 5: 157–169, 1998.

HILDEBRAND JG AND SHEPHERD GM. Mechanisms of olfactory discrimination: converging evidence for common principles across phyla. *Ann Rev Neurosci* 20: 595–631, 1997.

JOERGES J, KÜTTNER A, GALIZIA CG, AND MENZEL R. Representations of odours and odour mixtures visualized in the honeybee brain. *Nature* 387: 285–288, 1997.

KAWAHARA S, TODA S, SUZUKI Y, WATANABE S, AND KIRINO Y. Comparative study on neural oscillation in the procerebrum of the terrestrial slugs *Incilaria bilineata* and *Limax marginatus*. *J Exp Biol* 200: 1851–1861, 1997.

KIMURA T, SUZUKI H, KONO E, AND SEKIGUCHI T. Mapping of interneurons that contribute to food aversion conditioning in the slug brain. *Learn Mem* 4: 376–388, 1998a.

KIMURA T, TODA S, SEKIGUCHI T, KAWAHARA S, AND KIRINO Y. Optical recording analysis of olfactory response of the procerebral lobe in the slug brain. *Learn Mem* 4: 289–400, 1998b.

KIMURA T, TODA S, SEKIGUCHI T, AND KIRINO Y. Behavioral modulation induced by food odor aversive conditioning and its influence on the olfactory responses of an oscillatory brain network in the slug *Limax marginatus*. *Learn Mem* 4: 365–375, 1998c.

KLEINFELD D, DELANEY KR, FEE MS, FLORES JA, TANK DW, AND GELPERIN A. Dynamics of propagating waves in the olfactory network of a terrestrial mollusc: an electrical and optical study. *J Neurophysiol* 72: 1402–1419, 1994.

LAM YW, COHEN LB, WACHOWIAK M, AND ZOCHOWSKI MR. Odors elicit three different oscillations in the turtle olfactory bulb. *J Neurosci* 20: 749–762, 2000.

LI Z AND HOPFIELD JJ. Modeling the olfactory bulb and its neural oscillatory processings. *Biol Cybern* 61: 379–392, 1989.

LI Z AND HERTZ J. Odour recognition and segmentation by a model olfactory bulb and cortex. *Network* 11: 83–102, 2000.

LINSTER C AND GERVAIS R. Investigation of the role of interneurons and their modulation by centrifugal fibers in a neural model of the olfactory bulb. *J Comp Neurosci* 3: 225–246, 1996.

LLINAS R, RIBARY U, CONTRERAS D, AND PEDROARENA C. The neuronal basis of consciousness. *Philos Trans R Soc Lond B Biol Sci* 353: 1841–1849, 1998.

MANN-METZER P AND YAROM Y. Electronic coupling interacts with intrinsic properties to generate synchronized activity in cerebellar networks of inhibitory interneurons. *J Neurosci* 19: 3298–3306, 1999.

MARTIN KC AND KANDEL ER. Cell adhesion molecules, CREB, and the formation of new synaptic connections. *Neuron* 17: 567–570, 1996.

MELLON D AND WHELLER CJ. Coherent oscillations in membrane potential synchronize impulse bursts in central olfactory neurons of the crayfish. *J Neurophysiol* 81: 1231–1241, 1999.

MEREDITH M. Neural circuit computation-complex patterns in the olfactory bulb. *Brain Res Bull* 29: 111–117, 1992.

MURTHY VN AND FETZ EE. Oscillatory activity in sensorimotor cortex of awake monkeys: synchronization of local field potentials and relation to behavior. *J Neurophysiol* 76: 3949–3967, 1996.

PAGE E, GOINGS GE, UPSHAW-EARLEY J, AND HANCK DA. Endocytosis and uptake of Lucifer yellow by cultured atrial myocytes and isolated atria from adult rats. Regulation and subcellular localization. *Circ Res* 75: 335–346, 1994.

PESCHEL M, STRAUB V, AND TEYKE T. Consequences of food-attraction conditioning in *Helix*: a behavioral and electrophysiological study. *J Comp Physiol [A]* 178: 317–327, 1996.

SAHLEY C, GELPERIN A, AND RUDY JW. One-trial associative learning modifies food odor preferences of a terrestrial mollusc. *Proc Natl Acad Sci USA* 78: 640–642, 1981.

SARTHY PV, JOHNSON SM, AND DETWILER PB. Selective uptake of Lucifer yellow by retinal cells. *J Comp Neurol* 206: 371–378, 1982.

SEKIGUCHI T, YAMADA A, AND SUZUKI H. Reactivation dependent changes in memory states in the terrestrial slug *Limax flavus*. *Learn Mem* 4: 356–364, 1997.

SEKIGUCHI T, YAMADA A, SUZUKI H, AND MIZUKAMI A. Temporal analysis of the retention of a food-aversion conditioning in *Limax flavus*. *Zool Sci (Tokyo)* 8: 103–111, 1991.

SHEPHERD GM. Olfaction. In: *Fundamental Neuroscience*, edited by Zigmond MJ, Bloom FE, Landis SC, Roberts JL, and Squire LR. New York: Academic Press, 1999, p. 737–759.

SHIPLEY MT AND ENNIS M. Functional organization of olfactory system. *J Neurobiol* 30: 123–176, 1995.

SINGER W. Consciousness and the structure of neuronal representations. *Philos Trans R Soc Lond B Biol Sci* 353: 1829–1840, 1998.

SINGER W AND GRAY CM. Visual feature integration and the temporal correlation hypothesis. *Ann Rev Neurosci* 18: 555–586, 1995.

SQUIRE LR. *Memory and Brain.* New York: Oxford, 1987.

STOPFER M, BHAGAVAN S, SMITH BH, AND LAURENT G. Impaired odour discrimination on desynchronization of odour-encoding neural assemblies. *Nature* 390: 70–74, 1997.

TAYLOR JG AND KEVERNE EB. Accessory olfactory learning. *Biol Cybern* 64: 301–305, 1991.

TEYKE T. Nitric oxide, but not serotonin, is involved in acquisition of food-attraction conditioning in the snail *Helix pomatia*. *Neurosci Lett* 206: 29–32, 1996.

TEYKE T AND GELPERIN A. Olfactory oscillations augment odor discrimination not odor identification by *Limax* CNS. *Neuroreport* 10: 1061–1068, 1999.

TEYKE T, WANG JW, AND GELPERIN A. Lateralized memory storage and crossed inhibition during odor processing by *Limax*. *J Comp Physiol [A]* 186: 269–278, 2000.

VICKERS NJ, CHRISTENSEN TA, AND HILDEBRAND JG. Combinatorial odor discrimination in the brain: attractive and antagonistic odor blends are represented in distinct combinations of uniquely identifiable glomeruli. *J Comp Neurol* 400: 35–56, 1998.

WANG JW, DENK W, FLORES J, AND GELPERIN A. Initiation and propagation of calcium-dependent action potentials in a coupled network of olfactory interneurons. *J Neurophysiol* 85: 977–985, 2001.

WATANABE S, KAWAHARA S, AND KIRINO Y. Morphological chracterization of the bursting and nonbursting neurones in the olfactory centre of the terrestrial slug *Limax marginatus*. *J Exp Biol* 201: 925–930, 1998.

WEHR M AND LAURENT G. Relationship between afferent and central temporal patterns in the locust olfactory system. *J Neurosci* 19: 381–390, 1999.

WHITE J, HAMILTON KA, NEFF SR, AND KAUER JS. Emergent properties of odor information coding in a representational model of the salamander olfactory bulb. *J Neurosci* 12: 1772–1780, 1992.

WHITE JA, CHOW CC, RITT J, SOTO-TREVINO C, AND KOPELL N. Synchronization and oscillatory dynamics in heterogeneous mutually inhibited neurons. *J Comp Neurosci* 5: 5–17, 1998.

WUNDERER H, PICAUD S, AND FRANCESCHINI N. Selective illumination of single photoreceptors in the house fly retina: local turnover and uptake of extracellular horseradish peroxidase (HRP) and Lucifer yellow. *Cell Tissue Res* 257: 565–576, 1989.

YAMADA A, SEKIGUCHI T, SUZUKI H, AND MIZUKAMI A. Behavioral analysis of internal memory states using cooling-induced retrograde amnesia in *Limax flavus*. *J Neurosci* 12: 729–735, 1992.

ZAKHAROV IS, HAYES NL, IERUSALIMSKY VN, NOWAKOWSKI RS, AND BALABAN PM. Postembryonic neuronogenesis in the procerebrum of the terrestrial snail, *Helix lucorum*. *J Neurobiol* 35: 271–276, 1998.

ZIMMERMAN RP. Specific neuronal staining by in vitro uptake of Lucifer yellow. *Brain Res* 383: 287–298, 1986.

ZINKL GM, MAIER L, STUDER K, SAPP R, CHEN D-M, AND STARK WS. Microphotometric, ultrastructural, and electrophysiological analyses of light-dependent processes on visual receptors in white-eyed wild-type and norpA (no receptor potential) mutant *Drosophila*. *Vis Neurosci* 5: 429–439, 1990.